

Supplementary information

Visible light-driven enhanced CO₂ reduction by water over Cu modified S-doped g-C₃N₄

Niwesh Ojha, Abhinav Bajpai, Sushant Kumar*

Gas-Solid Interaction Laboratory, Department of Chemical and Biochemical Engineering,
Indian Institute of Technology Patna, Bihta, Patna, 801 106, Bihar, India

* Corresponding author:

(Sushant Kumar) E-mail: sushantkumar@iitp.ac.in; Tel.: +91-612-302-8670.

Fig. S1: XRD pattern of all the used catalysts and shifts in the (002) and (100) peaks after S and Cu loading onto the GCN.

Fig. S2: Plot between FWHM of the (002) peak and corresponding crystallite size (in nm) of the as-prepared catalysts

Fig. S3: Barrett-Joyner-Halenda (BJH) pore size distribution curves of GCN, SCN, and 2%Cu-SCN

Fig. S4: The EDX mapping of C, N, S, and Cu and the calculated mass ratio

Fig. S5: XPS survey scan of **(a)** GCN; **(b)** SCN; **(c)** 2% Cu-SCN

Fig. S6: The Tauc plot $(\alpha h\nu)^{1/2}$ against $h\nu$ curve for the as-synthesized catalysts

Table S1: The band gap energy (E_g) for the as-synthesized catalysts

Fig. S7: Schematic for experimental set up for gas-phase photocatalytic CO₂ reduction

Fig. S8: The gas chromatograph results of standard and different set of experiments

Fig. S9: Characterization of 2%Cu-SCN catalyst [(a) FTIR; (b) XRD; (c) FESEM used for four cycle of reaction

Fig. S10: Change in absorbance value of COO⁻ using second derivative

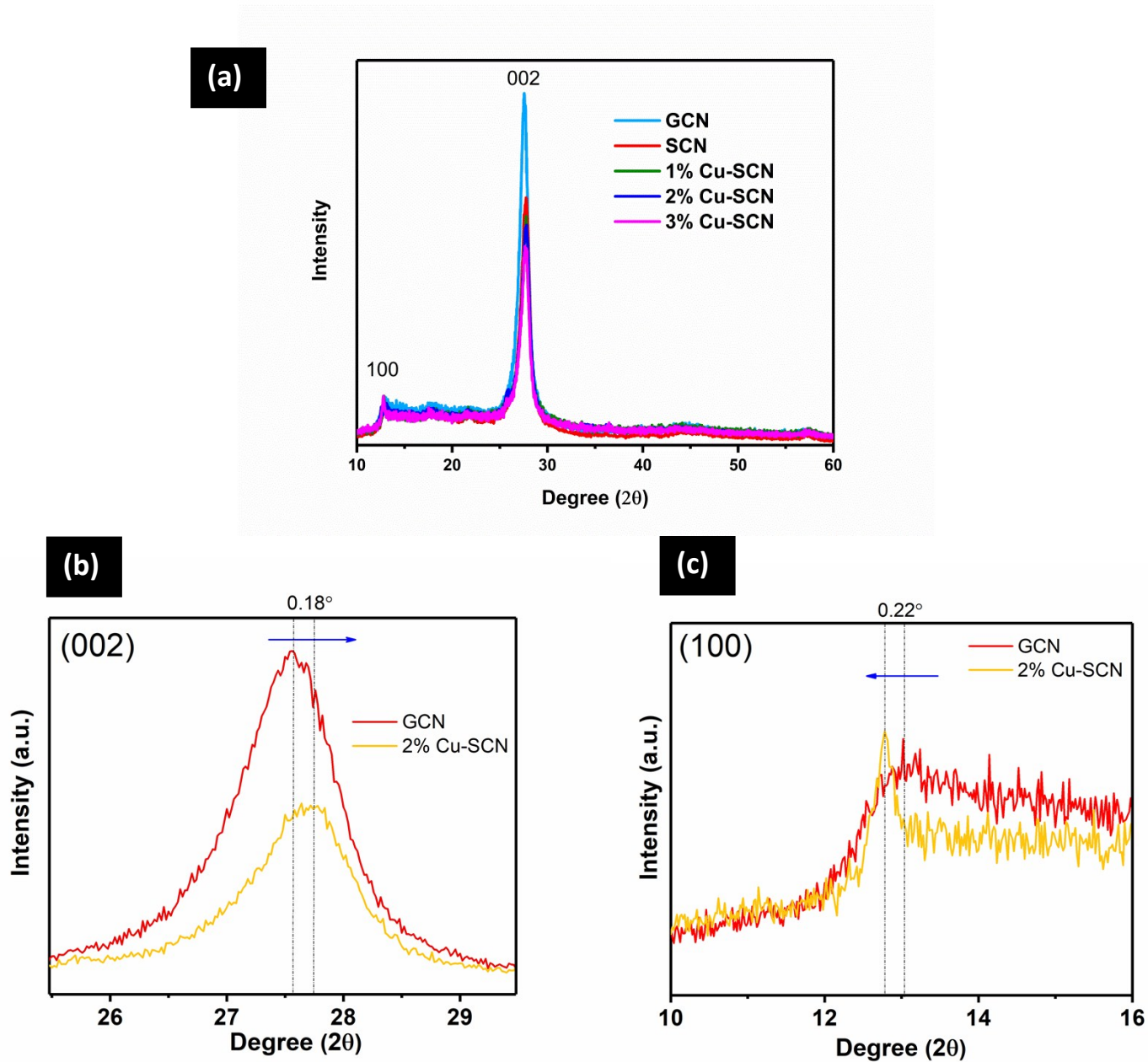


Figure S1 depicts (a) XRD pattern of all the used catalysts and also exhibits the shift in peak position of the (100) and (002). (b) A clear upshift in the (002) peak was observed for 2% Cu-SCN, which could be attributed to the reduction in inter-layer stacking distance of the pristine GCN. (c) Interestingly, a downshift in the (100) peak corresponds to increase in void-to-void distance of in-plane structure motifs. ¹

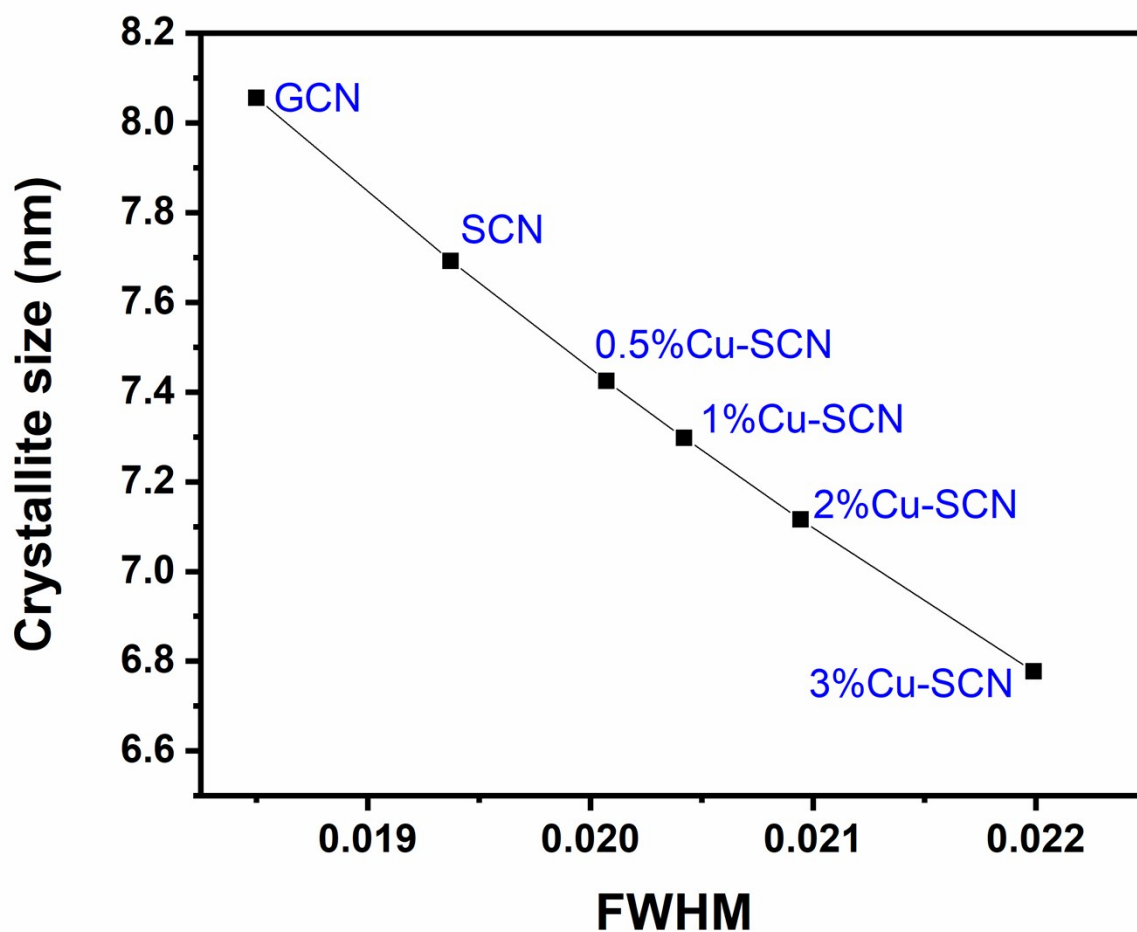


Figure S2. Plot between FWHM of the (002) peak and corresponding crystallite size (in nm) of the as-prepared catalysts. The crystallite size was calculated using the Scherrer's equation

$$\left[D = \frac{0.94 * \lambda_{Cu}}{FWHM * \cos(\theta)}; \lambda_{Cu} = 1.54\text{\AA} \right]$$

² The crystallite sizes have progressively reduced with increasing concentration of Cu in the catalysts.

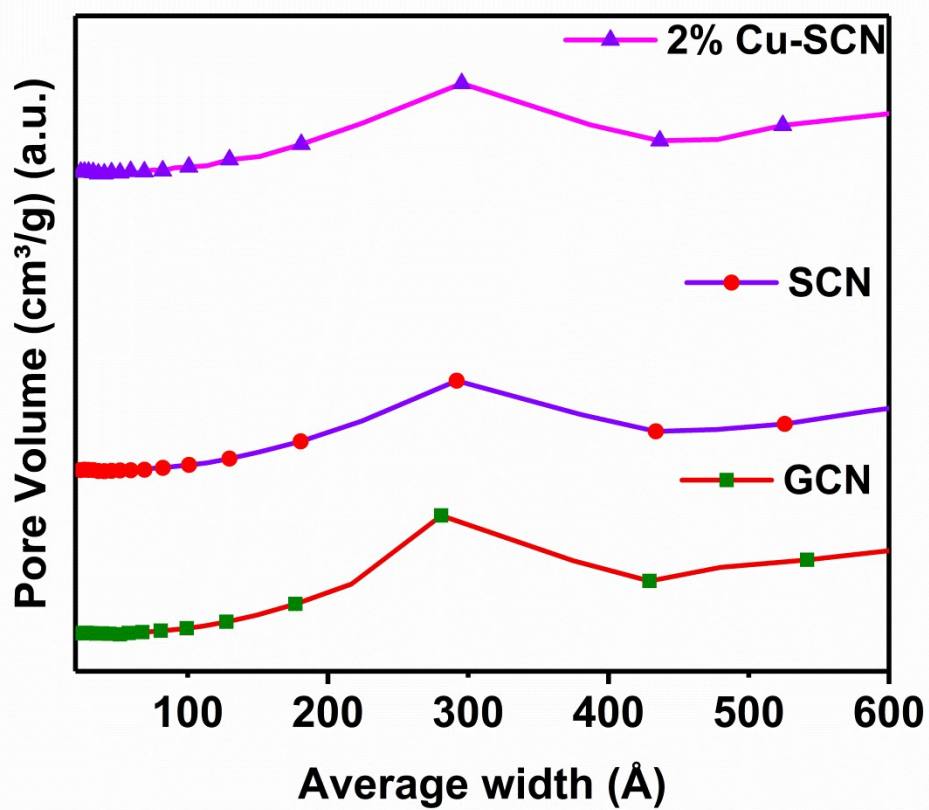


Figure S3. Barrett-Joyner-Halenda (BJH) pore size distribution curves of GCN, SCN, and 2%Cu-SCN. Here, the average pore width for all the catalysts lies in the range of (20-40) nm, which indicates that the catalysts were mesoporous.³

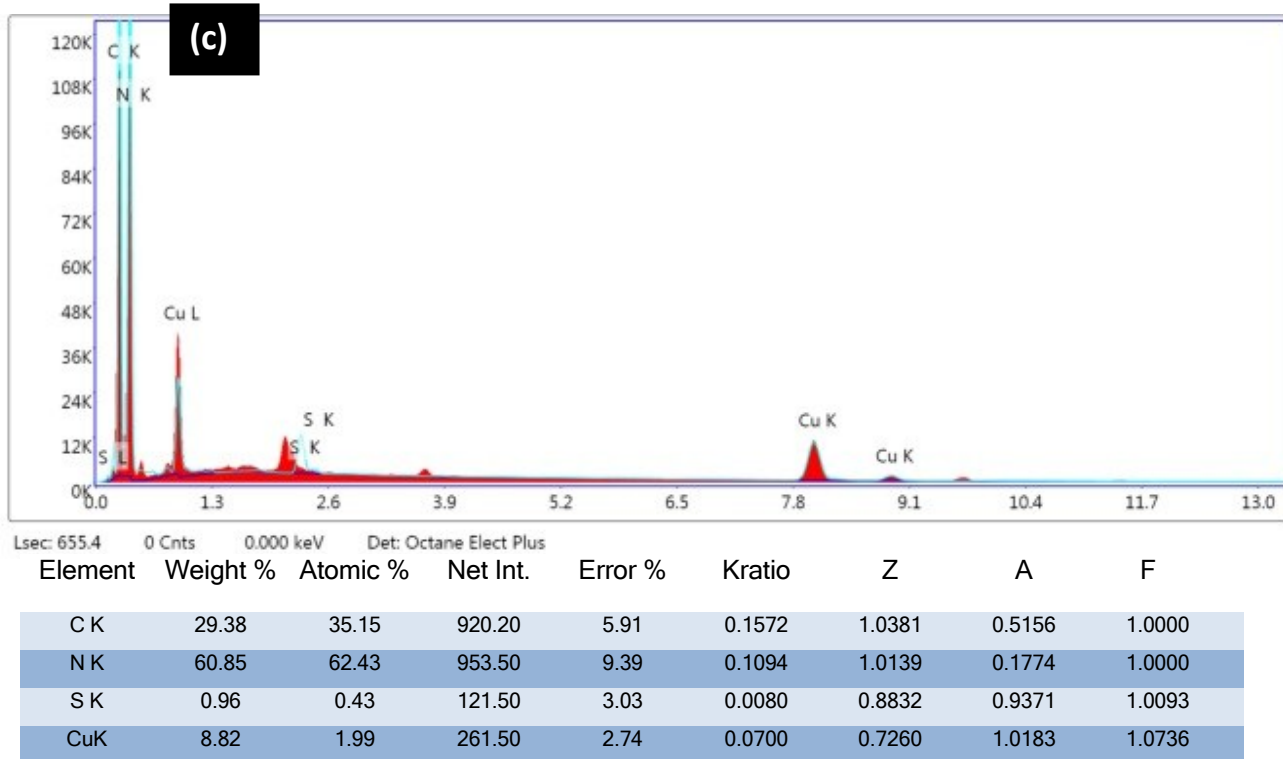
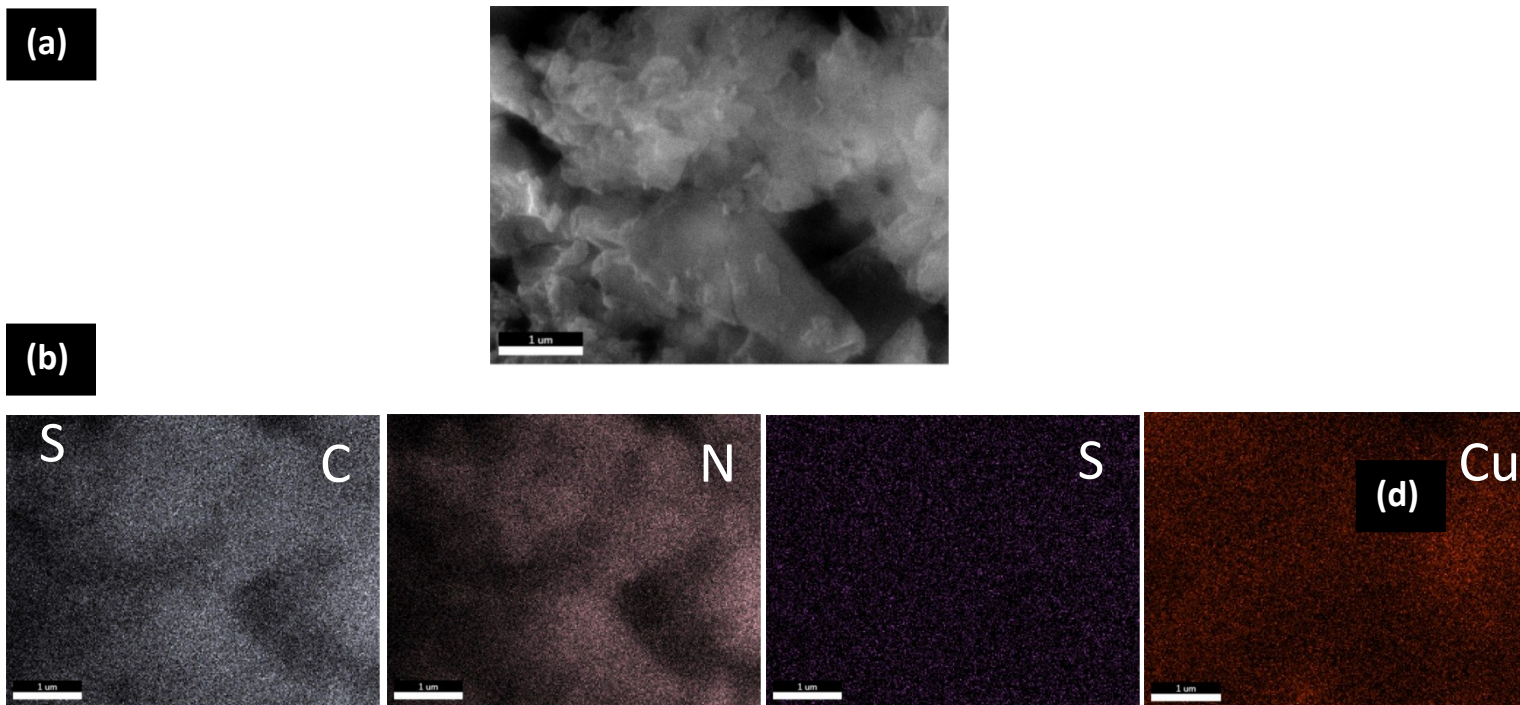


Figure S4. The EDX mapping images of 2% Cu-SCN catalyst: (a) SEM image; (b) EDX mapping of C, N, S, and Cu; (c) and (d) the calculated mass ratio. The result suggests that S and Cu are uniformly distributed in the catalyst.

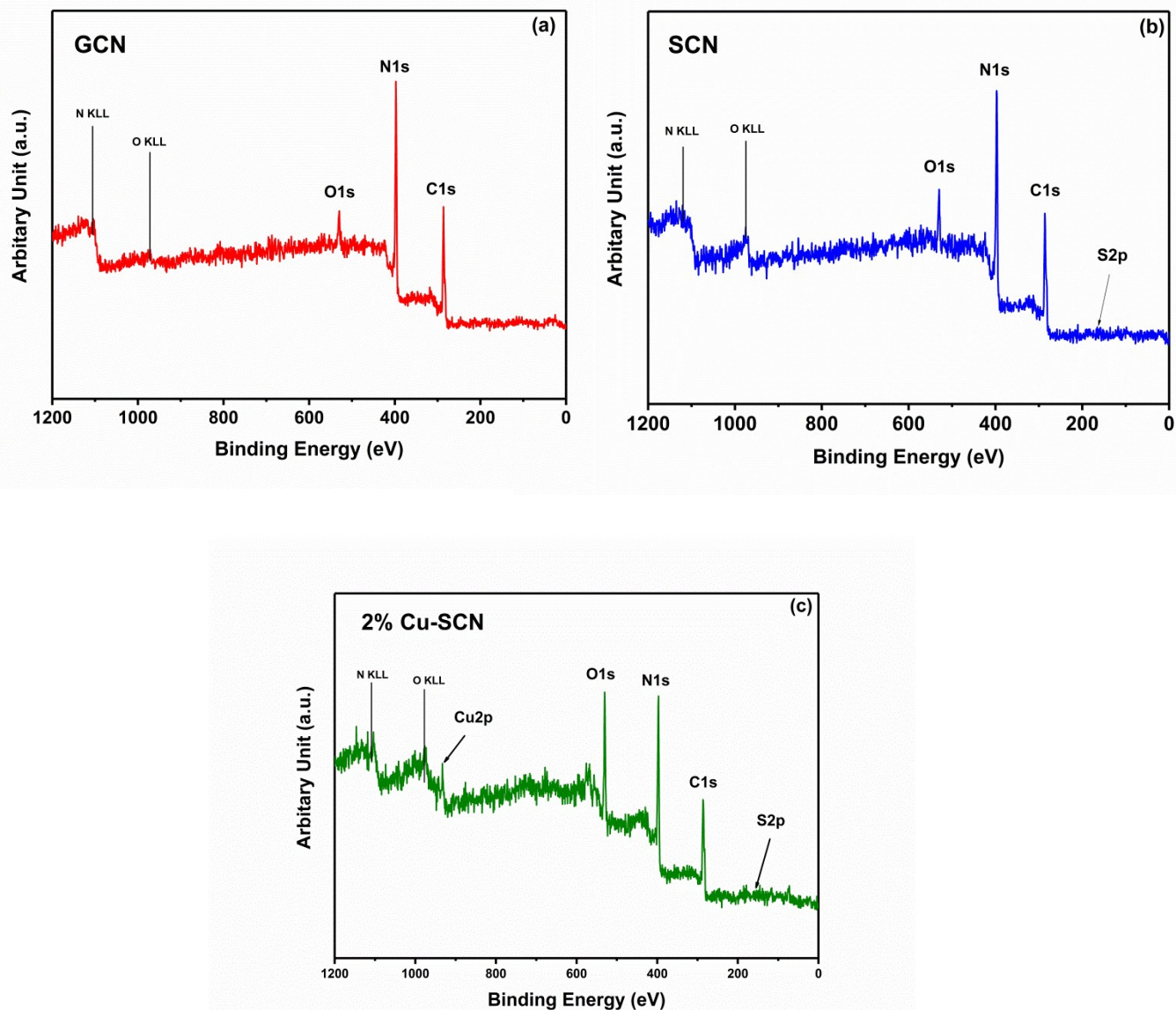


Figure S5. XPS survey scan of (a) GCN; (b) SCN; (c) 2% Cu-SCN. All scans show the existence of C, N, and surface oxygen. S and Cu are also present as shown in (c). Notably, Cu is in higher amount than S; this observation is in line with the EDX results [Figure S4].

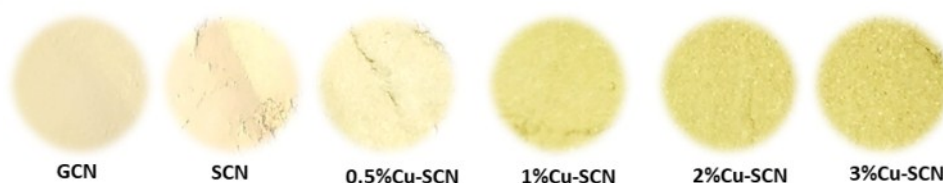
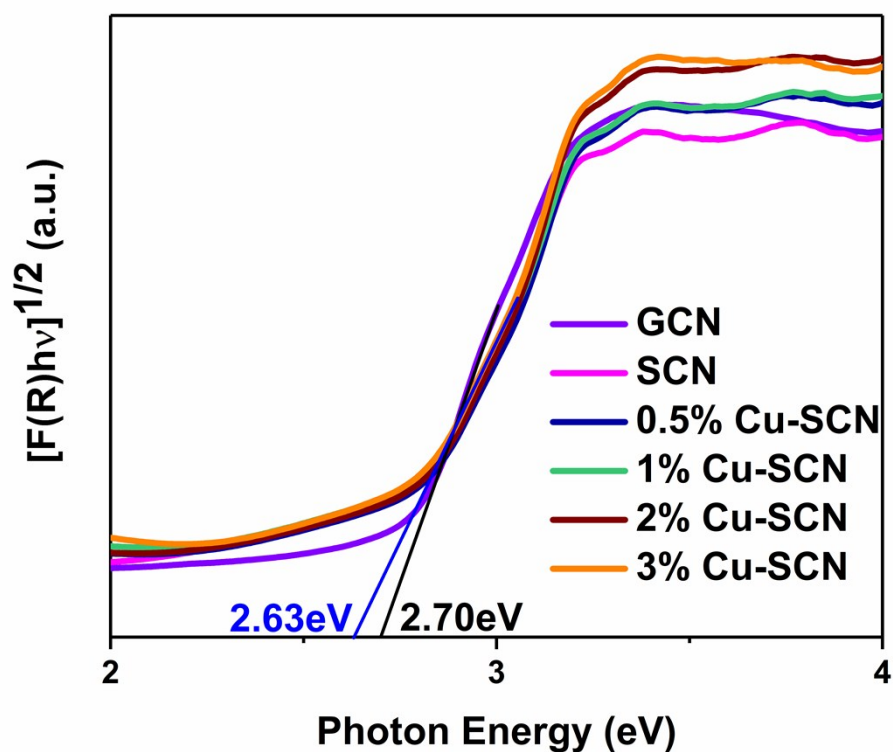


Figure S6. The Tauc plot $(\alpha h\nu)^{1/2}$ against $h\nu$ curve for the as-synthesized catalysts and their corresponding band gap energy (E_g) is illustrated in **Table S1**.^{4,5}

Table S1

Sample	Band Gap (eV)
GCN	2.70
SCN	2.63
0.5%Cu-SCN	2.63
1%Cu-SCN	2.63
2%Cu-SCN	2.63
3%Cu-SCN	2.69

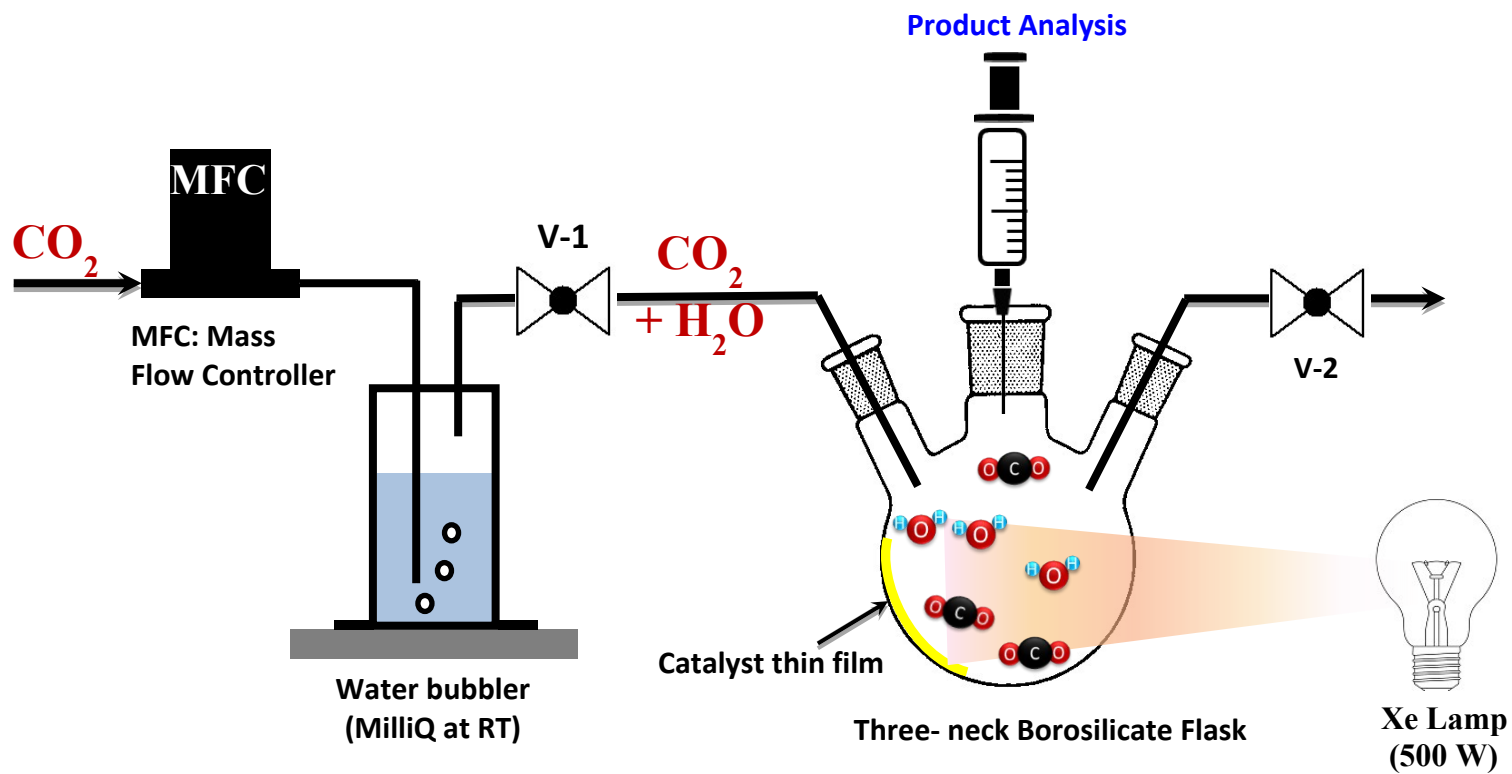
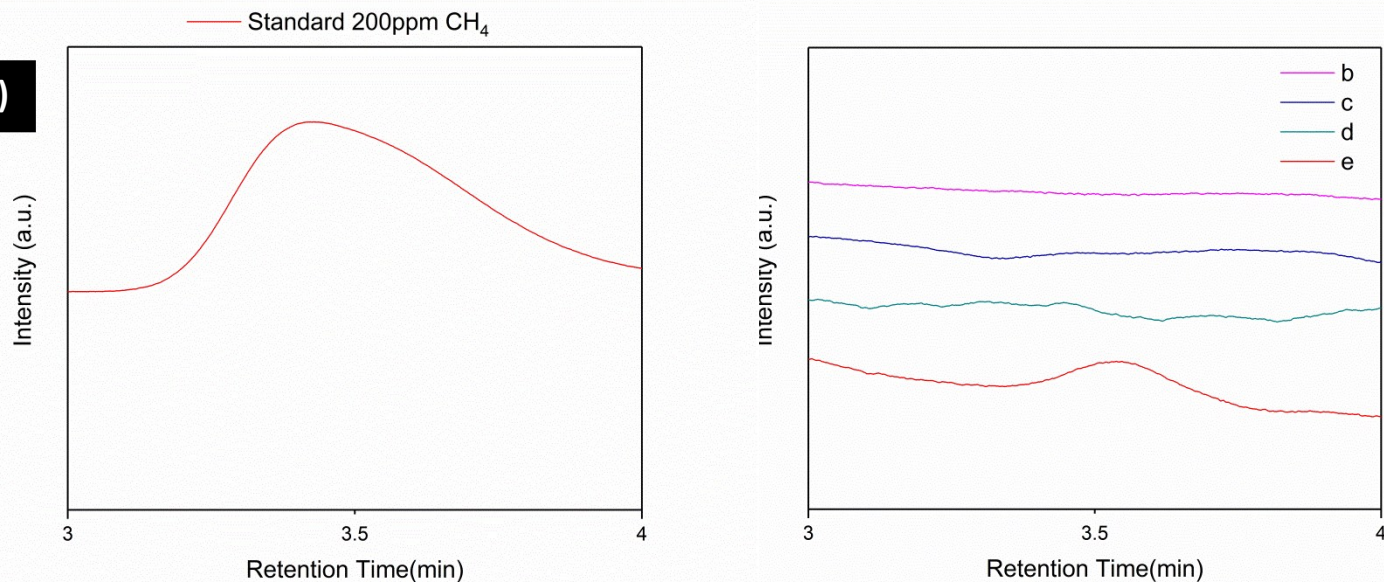


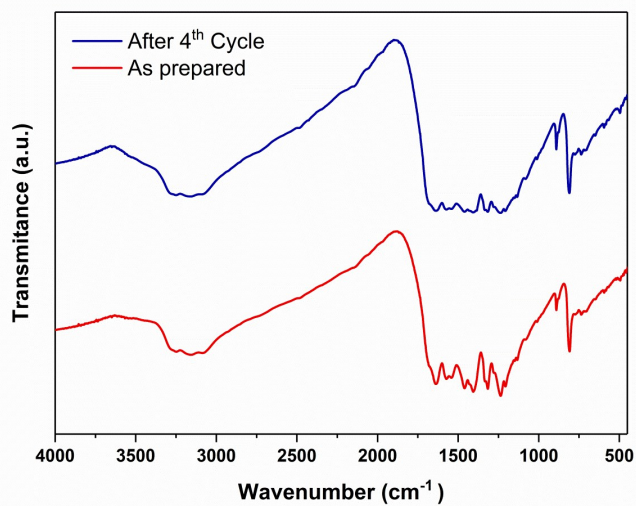
Figure S7. Schematic for experimental set up for gas-phase photocatalytic CO₂ reduction

(b)

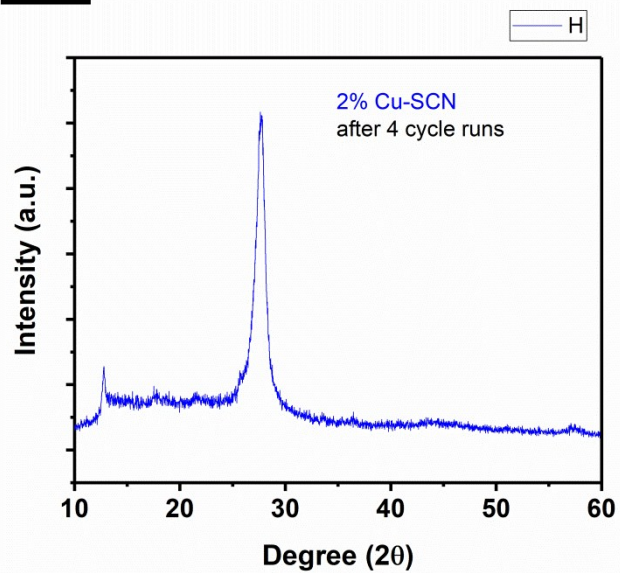
Experiment no. as listed above in (ii)	(CO ₂ + H ₂ O)	Photocatalyst	Irradiation
b	Yes	Yes	No
c	Yes	No	Yes
d	No	Yes	Yes
e	Yes	Yes	Yes

Figure S8. (a) (i) The gas chromatograph for 200ppm CH₄ present in the standard gas mixture. **(ii)** Gas chromatograph for different set of experiments, details of these experiments is tabulated in **(b)**. The graph in (ii) shows the successful formation of CH₄ (peak at ~3.5 min.) during the reaction. Moreover, it is evident that both photocatalyst and light irradiation are required to form the product (here, CO and CH₄).

(a)



(b)



(c)

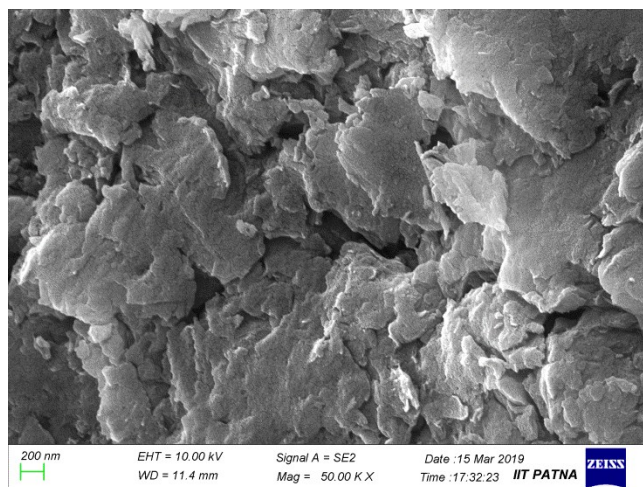
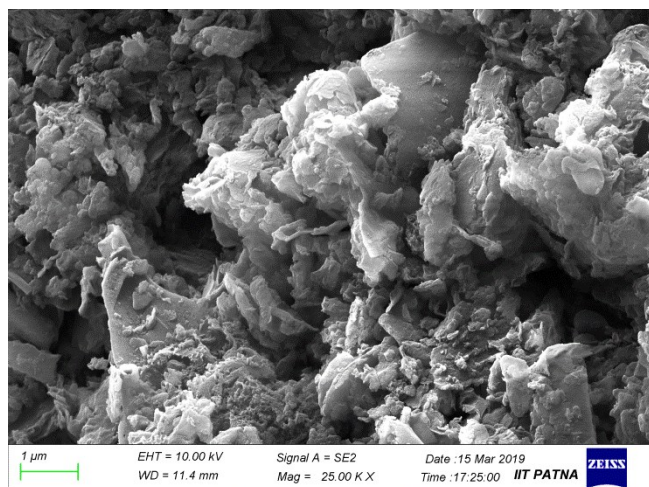


Figure S9. Characterization of 2%Cu-SCN catalyst used for four cycle of reaction: (a) FTIR spectra show no obvious spectral change was observed post-reaction; **(b)** Also, XRD pattern remains same and no new phase appears; **(c)** FESEM image shows that the planar structure of the catalyst remains intact even after four cycle of run (total = 16h).

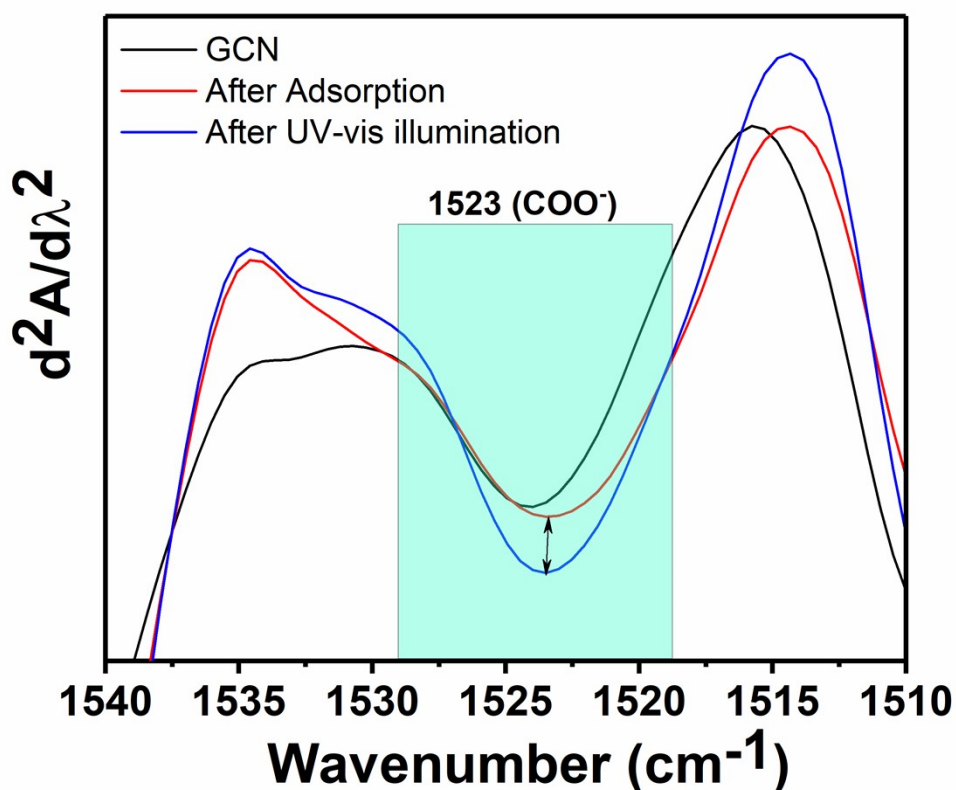


Figure S10 illustrates an enlarged portion of the IR spectrum in wavenumber range of 1540-1510 cm^{-1} . The plot shows change in absorbance value of COO⁻ using second derivative. Here, the absorbance value for GCN and after adsorption remains almost same. Upon light irradiation,

there is an apparent change in the absorbance value which clearly confirms the formation of COO^- ; an activated form of CO_2 that primarily initiates the CO_2 photo-reduction process.

References:

- 1 L. Shi, L. Liang, F. Wang, J. Ma and J. Sun, *Catal. Sci. Technol*, 2014, **4**, 3235.
- 2 P. Reñones, A. Moya, F. Fresno, L. Collado, J. J. Vilatela and V. A. de la Peña O'Shea, *Journal of CO2 Utilization*, 2016, **15**, 24–31.
- 3 S. Sun, X. Gou, S. Tao, J. Cui, J. Li, Q. Yang, S. Liang and Z. Yang, *Mater. Chem. Front*, 2019, **3**, 597.
- 4 J. Liu, Y. Yu, R. Qi, C. Cao, X. Liu, Y. Zheng and W. Song, *Applied Surface Science*, 2019, **244**, 459-464.
- 5 P. Wu, J. Wang, J. Zhao, L. Guo and F. E. Osterloh, *J. Mater. Chem. A*, 2014, **2**, 20338-20344 .